Hindawi
Advances in High Energy Physics
Volume 2018, Article ID 8523854, 16 pages
https://doi.org/10.1155/2018/8523854

Research Article

Z' and Higgs Boson Production Associated with a Top Quark Pair as a Probe of the $U(1)_{B-L}$ Model at e^+e^- Colliders

F. Ramírez-Sánhez,[1] A. Gutiérrez-Rodríguez [1], Alejandro González-Sánchez,[1,2] and M. A. Hernández-Ruíz[3]

[1] *Facultad de Física, Universidad Autónoma de Zacatecas, Apartado Postal C-580, 98060 Zacatecas, Mexico*
[2] *Departamento de Investigación, Universidad Popular Autónoma del Estado de Puebla, 21 Sur 1103, Col. Santiago, C. P. 72410, Puebla, Mexico*
[3] *Unidad Académica de Ciencias Químicas, Universidad Autónoma de Zacatecas, Apartado Postal C-585, 98060 Zacatecas, Mexico*

Correspondence should be addressed to A. Gutiérrez-Rodríguez; alexgu@fisica.uaz.edu.mx

Received 17 December 2017; Revised 4 May 2018; Accepted 21 May 2018; Published 3 July 2018

Academic Editor: Enrico Lunghi

We study the production sensitivity of Higgs bosons h and H, in relation to the possible existence of Z' boson and a top quark pair at the energy scales that will be reached in the near future at projected e^+e^- linear colliders. We focus on the resonance and no-resonance effects of the annihilation processes $e^+e^- \longrightarrow (\gamma, Z, Z') \longrightarrow t\bar{t}h$ and $e^+e^- \longrightarrow (\gamma, Z, Z') \longrightarrow t\bar{t}H$. Furthermore, we develop and present novel analytical formulas to assess the total cross section involved in the production of Higgs bosons. We find that the possibility of performing precision measurements for the Higgs bosons h and H and for the Z' boson is very promising at future e^+e^- linear colliders.

1. Introduction

The Compact Linear Collider (CLIC) [1–3] is e^+e^- machine that operates at a center-of-mass energy of $0.5 - 3\ TeV$ and luminosities within $\mathscr{L} = 500 - 2000\ fb^{-1}$. This makes it a powerful tool to perform high precision studies of the properties of the Higgs boson in the Standard Model (SM) [4–8] and of new particles predicted by other extended models, such as the case of the $SU(3)_C \times SU(2)_L \times U(1)_Y \times U(1)_{B-L}$ (B-L) theory given in [9–14], which is the benchmark model and the starting point for our research. In the extended gauge sector, the B-L model contains an extra gauge boson Z' and an additional heavy neutral Higgs boson H, and the theory predicts the existence of heavy neutrinos ν_R. These three elements altogether make the model phenomenologically interesting. With its great capability to cover ample energy scales, one primary goal of the CLIC is to directly search for new particles, especially those coupled to SM particles. In addition, the CLIC can potentially produce directly new particles that could modify the Higgs properties. The CLIC can significantly improve the Large Hadron Collider (LHC) measurements due to its clean environment.

High-energy colliders benefit the high rate production of top-Higgs via the processes $e^+e^- \longrightarrow t\bar{t}h$ and $e^+e^- \longrightarrow t\bar{t}H$. This is crucial to directly constrain the top Yukawa coupling, and it helps us to decipher the Higgs boson properties and to give light to new physics beyond the SM. The production of a Higgs boson in association with top quarks requires a large center-of-mass energy which is achieved at a linear collider as is the case of the CLIC. The Higgs boson in association with a top quark pair can be produced at other colliders, such as the LHC and the International Linear Collider (ILC) at $\sqrt{s} = 500\ GeV$, albeit in the former the main process occurs through gluon splitting.

In this paper, we study the simple production of Higgs bosons h, H associated with the underlying Z' resonance, and a top quark pair via the processes $e^+e^- \longrightarrow (\gamma, Z, Z') \longrightarrow t\bar{t}h$ and $e^+e^- \longrightarrow (\gamma, Z, Z') \longrightarrow t\bar{t}H$ in the context of the B-L model [9–16]. Hereafter, we denote the Higgs bosons h and H in the SM and in the B-L model, respectively. We derive

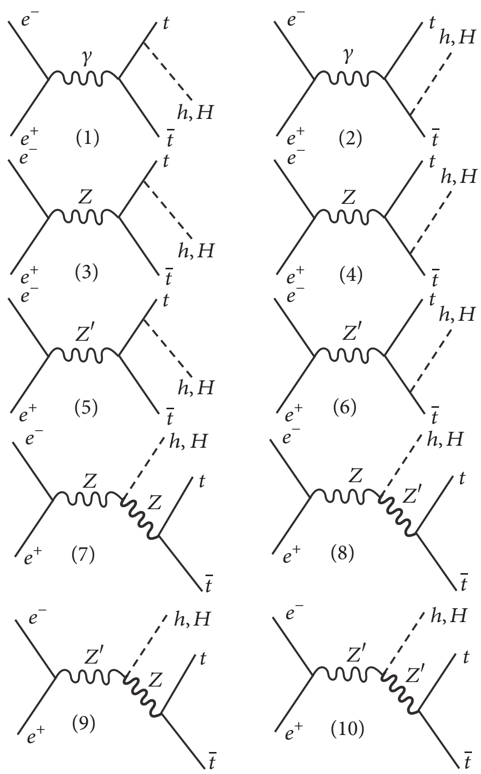

Figure 1: Feynman diagrams for the Higgs bosons production in association with $t\bar{t}$ pair $e^+e^- \longrightarrow t\bar{t}h$ and $e^+e^- \longrightarrow t\bar{t}H$ in the B-L model.

complete analytical expressions for (i) the decays of the new heavy gauge boson Z' to three bodies $\Gamma(Z' \longrightarrow f\bar{f}h, f\bar{f}H)$ and (ii) analytical formulas for the total cross section of the processes $e^+e^- \longrightarrow (\gamma, Z, Z') \longrightarrow t\bar{t}h, t\bar{t}H$. Thus, our analytical results of the Higgs bosons production and decay can easily be implemented in searching for signatures of new physics and could be of scientific significance. The Feynman diagrams contributing to the processes $e^+e^- \longrightarrow (\gamma, Z, Z') \longrightarrow t\bar{t}h, t\bar{t}H$ are shown in Figure 1.

The structure of our paper is as follows. In Section 2, we give a brief review of the B-L model. In Section 3, we calculate the decay widths of the heavy gauge boson Z' for the three body processes. Then, we present the calculation of the cross section for the processes $e^+e^- \longrightarrow (\gamma, Z, Z') \longrightarrow t\bar{t}h, t\bar{t}H$ in Section 4 and our results and conclusions are presented in Section 5.

2. Brief Review of the B-L Model

Here, we consider the simple extension of the SM [9–11, 15, 17–23] of the form $SU(3)_C \times SU(2)_L \times U(1)_Y \times U(1)_{B-L}$, where $U(1)_{B-L}$, represents the additional gauge symmetry. The gauge invariant Lagrangian of this model is given by

$$\mathscr{L} = \mathscr{L}_s + \mathscr{L}_{YM} + \mathscr{L}_f + \mathscr{L}_Y, \tag{1}$$

where $\mathscr{L}_s, \mathscr{L}_{YM}, \mathscr{L}_f$, and $\mathscr{L}_Y$ are the scalar, Yang-Mills, fermion, and Yukawa sectors, respectively.

Next, we briefly describe the Lagrangian including the scalar, fermion, and gauge sectors. The Lagrangian for the gauge sector is given by [9, 22, 24, 25]

$$\mathscr{L}_g = -\frac{1}{4}B_{\mu\nu}B^{\mu\nu} - \frac{1}{4}W^a_{\mu\nu}W^{a\mu\nu} - \frac{1}{4}Z'_{\mu\nu}Z'^{\mu\nu}, \tag{2}$$

$W^a_{\mu\nu}$, $B_{\mu\nu}$, and $Z'_{\mu\nu}$ being the field strength tensors for $SU(2)_L$, $U(1)_Y$, and $U(1)_{B-L}$. The scalar Lagrangian for this model can be written as

$$\mathscr{L}_s = (D^\mu\Phi)^\dagger \left(D_\mu\Phi\right) + (D^\mu\chi)^\dagger \left(D_\mu\chi\right) - V(\Phi, \chi), \tag{3}$$

and the most general Higgs potential invariant of gauge is given by [21]

$$\begin{aligned} V(\Phi, \chi) = {} & m^2 \left(\Phi^\dagger\Phi\right) + \mu^2 |\chi|^2 + \lambda_1 \left(\Phi^\dagger\Phi\right)^2 + \lambda_2 |\chi|^4 \\ & + \lambda_3 \left(\Phi^\dagger\Phi\right) |\chi|^2, \end{aligned} \tag{4}$$

with Φ and χ as the complex scalar Higgs doublet and singlet fields. The covariant derivative is given by [19–21]

$$\begin{aligned} D_\mu = {} & \partial_\mu + ig_s t^\alpha G^\alpha_\mu \\ & + i\left[gT^a W^a_\mu + g_1 Y B_\mu + \left(\tilde{g}Y + g'_1 Y_{B-L}\right) B'_\mu\right], \end{aligned} \tag{5}$$

where g_s, g, g_1, and g'_1 are the $SU(3)_C$, $SU(2)_L$, $U(1)_Y$, and $U(1)_{B-L}$ couplings with t^α, T^a, Y, and Y_{B-L} being their corresponding group generators.

After spontaneous symmetry breaking, the two scalar fields can be written as

$$\begin{aligned} \Phi &= \begin{pmatrix} 0 \\ \dfrac{v + \phi^0}{\sqrt{2}} \end{pmatrix}, \\ \chi &= \frac{v' + \phi'^0}{\sqrt{2}}, \end{aligned} \tag{6}$$

with $v \approx 246\ GeV$ and v' being the electroweak and B-L symmetry breaking scales, respectively. These are real and positive valuated scales. Getting the minima of the Higgs potential, (4) gives the scalar mass eigenvalues ($M_H > M_h$)

$$M^2_{H,h} = \lambda_1 v^2 + \lambda_2 v'^2 \pm \sqrt{\left(\lambda_1 v^2 - \lambda_2 v'^2\right)^2 + \lambda_3^2 v^2 v'^2}, \tag{7}$$

and the mass eigenstates are linear combinations of ϕ^0 and ϕ'^0 and written as

$$\begin{pmatrix} h \\ H \end{pmatrix} = \begin{pmatrix} \cos\alpha & -\sin\alpha \\ \sin\alpha & \cos\alpha \end{pmatrix} \begin{pmatrix} \phi^0 \\ \phi'^0 \end{pmatrix}, \tag{8}$$

where the scalar mixing angle α ($-\pi/2 \leq \alpha \leq \pi/2$) can be expressed as

$$\tan(2\alpha) = \frac{\lambda_3 v v'}{\lambda_2 v'^2 - \lambda_1 v^2}, \tag{9}$$

while coupling constants λ_1, λ_2, and λ_3 are determined using (7)-(9).

Interpreting the LHC data [26, 27] by identifying h with the recently observed Higgs boson, the scalar field mixing angle satisfies the constraint $\sin^2\alpha \lesssim 0.33(0.36)$ for $M_H = 200(300)$ GeV as discussed in [28, 29].

In analogy with the SM, the fields of definite mass are linear combinations of B^μ, W_3^μ, and B'^μ; the relation between the neutral gauge bosons (B^μ, W_3^μ and B'^μ) and the corresponding mass eigenstates are given by [11, 12, 19, 20]

$$\begin{pmatrix} B^\mu \\ W^{3\mu} \\ B'^\mu \end{pmatrix} = \begin{pmatrix} \cos\theta_W & -\sin\theta_W\cos\theta' & \sin\theta_W\sin\theta' \\ \sin\theta_W & \cos\theta_W\cos\theta' & -\cos\theta_W\sin\theta' \\ 0 & \sin\theta' & \cos\theta' \end{pmatrix} \begin{pmatrix} A^\mu \\ Z^\mu \\ Z'^\mu \end{pmatrix}, \quad (10)$$

with $-\pi/4 \le \theta' \le \pi/4$, such that

$$\tan 2\theta' = \frac{2\tilde{g}\sqrt{g^2+g_1^2}}{\tilde{g}^2 + 16\left(\nu'/\nu\right)^2 g_1'^2 - g^2 - g_1^2}. \quad (11)$$

From the corresponding Lagrangian for the $SU(3)_C \times SU(2)_L \times U(1)_Y \times U(1)_{B-L}$ model, the interaction terms between neutral gauge bosons Z, Z' and a pair of fermions of the SM can be written in the form [9, 10, 14, 30, 31]

$$\begin{aligned}\mathscr{L}_{NC} = {} & \frac{-ig}{\cos\theta_W}\sum_f \bar{f}\gamma^\mu \frac{1}{2}\left(g_V^f - g_A^f\gamma^5\right) f Z_\mu \\ & + \frac{-ig}{\cos\theta_W}\sum_f \bar{f}\gamma^\mu \frac{1}{2}\left(g_V'^f - g_A'^f\gamma^5\right) f Z'_\mu. \end{aligned} \quad (12)$$

From the latter we determine the expressions for the new couplings of the Z, Z' bosons with the SM fermions, which are given in Table 2 of [13, 14]. The couplings $g_V^f(g_V'^f)$ and $g_A^f(g_A'^f)$ depend on the $Z - Z'$ mixing angle $\theta\prime$ and the coupling constant g_1' of the B-L interaction. In these couplings, the current bound on the mixing angle is $|\theta'| \le 10^{-3}$ [32–35]. The couplings of the SM are recovered in the limit, when $\theta' = 0$ and $g_1' = 0$.

3. The Decay Widths of the Underlying Z' Boson

The relevant decay widths of the Z' boson for the two body processes are presented in [13, 14]. The Z' partial decay widths for the three body processes $\Gamma(Z' \longrightarrow f\bar{f}h, f\bar{f}H)$ and $\Gamma(Z' \longrightarrow W^+W^-h, W^+W^-H)$ are given by

$$\begin{aligned}\Gamma\left(Z' \longrightarrow f\bar{f}h, f\bar{f}H\right) &= \frac{G_F M_Z^2 M_{Z'}}{32\pi^3}\left[\Gamma_1\left(g_V'^f, g_A'^f, x_1, x_2\right)\right. \\ &\quad \left. + \Gamma_2\left(g_V'^f, g_A'^f, x_1, x_2\right) + \Gamma_3\left(g_V'^f, g_A'^f, x_1, x_2\right)\right], \end{aligned} \quad (13)$$

and

$$\begin{aligned}\Gamma\left(Z' \longrightarrow W^+W^-h, W^+W^-H\right) &= \frac{G_F^2 M_{Z'}^3 M_W^2 \cos^2\theta_W \sin^2\theta' \left(\cos^2\alpha, \sin^2\alpha\right)}{8\pi^3} \\ &\quad \times \left[\Gamma_4\left(x_1,x_2\right) + \Gamma_5\left(x_1,x_2\right) + \Gamma_6\left(x_1,x_2\right)\right]. \end{aligned} \quad (14)$$

Full and explicit expressions for the $\Gamma_i(g_V'^f, g_A'^f, x_1, x_2)$ and $\Gamma_i(x_1, x_2)$, $i = 1, 2, \ldots, 6$, together with the corresponding limits of integration are given in Appendix A.

4. Higgs Boson Production Associated with a Top Quark Pair

We now proceed to calculate the total cross section of the processes $e^+e^- \longrightarrow t\bar{t}h, t\bar{t}H$. The Feynman diagrams contributing to the processes $e^+e^- \longrightarrow (\gamma, Z, Z') \longrightarrow t\bar{t}h, t\bar{t}H$ are shown in Figure 1.

We express the total cross section of the processes mentioned before in compact form as a sum of the different contributions; that is,

$$\begin{aligned}\sigma_{Tot}\left(e^+e^- \longrightarrow t\bar{t}h, t\bar{t}H\right) &= \sigma_\gamma\left(e^+e^- \longrightarrow t\bar{t}h, t\bar{t}H\right) + \sigma_Z\left(e^+e^- \longrightarrow t\bar{t}h, t\bar{t}H\right) \\ &\quad + \sigma_{Z'}\left(e^+e^- \longrightarrow t\bar{t}h, t\bar{t}H\right) \\ &\quad + \sigma_{\gamma,Z}\left(e^+e^- \longrightarrow t\bar{t}h, t\bar{t}H\right) \\ &\quad + \sigma_{\gamma,Z'}\left(e^+e^- \longrightarrow t\bar{t}h, t\bar{t}H\right) \\ &\quad + \sigma_{Z,Z'}\left(e^+e^- \longrightarrow t\bar{t}h, t\bar{t}H\right), \end{aligned} \quad (15)$$

where

$$\sigma_\gamma\left(e^+e^- \longrightarrow t\bar{t}h, t\bar{t}H\right) = \frac{G_F^2 M_Z^4}{\pi^2 s} \cdot \int_{x_1^-}^{x_1^+}\int_{x_2^-}^{x_2^+} Q_e^2 Q_t^2 I_1\left(x_1,x_2\right) dx_1 dx_2, \quad (16)$$

$$\begin{aligned}\sigma_Z\left(e^+e^- \longrightarrow t\bar{t}h, t\bar{t}H\right) &= \frac{G_F^2 M_Z^4 s}{\pi^2} \cdot \int_{x_1^-}^{x_1^+}\int_{x_2^-}^{x_2^+} \frac{\left(g_V^{e2} + g_A^{e2}\right)}{\left[\left(s - M_Z^2\right)^2 + M_Z^2\Gamma_Z^2\right]} \times \left[\left(g_V^{t2} + g_A^{t2}\right)\right. \\ &\quad \cdot I_1\left(x_1,x_2\right) + g_A^{t2}\sum_{i=2}^{6} I_i\left(x_1,x_2\right) + g_V^{t2}\left(I_4\left(x_1,x_2\right)\right. \\ &\quad \left.\left. + I_6\left(x_1,x_2\right)\right)\right] \times dx_1 dx_2, \end{aligned} \quad (17)$$

$$\sigma_{Z'}\left(e^+e^- \longrightarrow t\bar{t}h, t\bar{t}H\right) = \frac{G_F^2 M_Z^4 s}{\pi^2} \cdot \int_{x_1^-}^{x_1^+}\int_{x_2^-}^{x_2^+} \frac{\left(g_V^{\prime e2} + g_A^{\prime e2}\right)}{\left[\left(s - M_{Z'}^2\right)^2 + M_{Z'}^2\Gamma_{Z'}^2\right]} \times \left[\left(g_V^{\prime t2} + g_A^{\prime t2}\right) I_1\left(x_1, x_2\right) + g_A^{\prime t2}\sum_{i=7}^{10} I_i\left(x_1, x_2\right) + g_V^{\prime t2}\left(I_8\left(x_1, x_2\right) + I_{10}\left(x_1, x_2\right)\right)\right] \times dx_1 dx_2, \quad (18)$$

$$\sigma_{\gamma,Z}\left(e^+e^- \longrightarrow t\bar{t}h, t\bar{t}H\right) = \frac{G_F^2 M_Z^4}{\pi^2} \cdot \int_{x_1^-}^{x_1^+}\int_{x_2^-}^{x_2^+} \frac{Q_e Q_t g_V^e g_V^t}{\left[\left(s - M_Z^2\right) + M_Z\Gamma_Z\right]} \times \left[2I_1\left(x_1, x_2\right) + I_6\left(x_1, x_2\right)\right] dx_1 dx_2, \quad (19)$$

$$\sigma_{\gamma,Z'}\left(e^+e^- \longrightarrow t\bar{t}h, t\bar{t}H\right) = \frac{G_F^2 M_Z^4}{\pi^2} \cdot \int_{x_1^-}^{x_1^+}\int_{x_2^-}^{x_2^+} \frac{Q_e Q_t g_V^{\prime e} g_V^{\prime t}}{\left[\left(s - M_{Z'}^2\right) + M_{Z'}\Gamma_{Z'}\right]} \times \left[2I_1\left(x_1, x_2\right) + I_{10}\left(x_1, x_2\right)\right] dx_1 dx_2, \quad (20)$$

$$\sigma_{Z,Z'}\left(e^+e^- \longrightarrow t\bar{t}h, t\bar{t}H\right) = \frac{2G_F^2 M_Z^4}{\pi^2 s} \cdot \int_{x_1^-}^{x_1^+}\int_{x_2^-}^{x_2^+} \left(g_V^e g_V^{\prime e} + g_A^e g_A^{\prime e}\right) \times \frac{\left[\left(s - M_Z^2\right)\left(s - M_{Z'}^2\right) + M_Z M_{Z'}\Gamma_Z\Gamma_{Z'}\right]}{\left[\left(s - M_Z^2\right)^2 + M_Z^2\Gamma_Z^2\right]\left[\left(s - M_{Z'}^2\right)^2 + M_{Z'}^2\Gamma_{Z'}^2\right]} \times \left[\left(g_V^t g_V^{\prime t} + g_A^t g_A^{\prime t}\right) I_1\left(x_1, x_2\right) + \left(g_A^t g_A^{\prime t}\right) \cdot \sum_{i=2}^{10} I_i\left(x_1, x_2\right) + \left(g_V^t g_V^{\prime t}\right)\left(I_4\left(x_1, x_2\right) + I_6\left(x_1, x_2\right) + I_8\left(x_1, x_2\right) + I_{10}\left(x_1, x_2\right)\right)\right] dx_1 dx_2. \quad (21)$$

The explicit form of the functions $I_i(x_1, x_2)$, $i = 1, 2, \ldots, 10$, and of their corresponding limits of integration $x_1^{\pm}(x_2^{\pm})$ are given in Appendices A and B.

Eqs. (16) and (17) determine the cross section with the exchange of the γ photon and the Z boson, while the expressions in (18)-(21) quantify the cross section contributions of the B-L model and of the interference, respectively. The expression for the cross section of the reaction $e^+e^- \longrightarrow t\bar{t}h$ in the SM can easily be recovered in the decoupling limits $\theta' = 0$, $g_1' = 0$ and $\alpha = 0$. Thus (15) reduces to the SM [41–45].

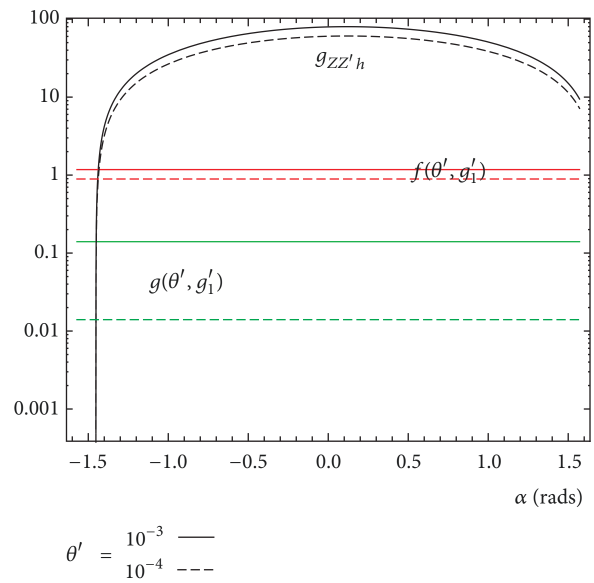

FIGURE 2: $g_{ZZ'h}(\theta', g_1')$ coupling and $f(\theta', g_1')$, $g(\theta', g_1')$ functions as a function of α.

5. Results and Conclusions

We have addressed a study of the total cross section $\sigma_{Tot} = \sigma_{Tot}(\sqrt{s}, M_{Z'}, g_1', \theta', \alpha)$ for the processes of simple Higgs bosons production $e^+e^- \longrightarrow (\gamma, Z, Z') \longrightarrow t\bar{t}h$ and $e^+e^- \longrightarrow (\gamma, Z, Z') \longrightarrow t\bar{t}H$ in association with the underlying Z' boson and a top quark pair within the context of the $SU(3)_C \times SU(2)_L \times U(1)_Y \times U(1)_{B-L}$ model [9–14]. This has been done as a function of the parameters of the model, which will be used by the CLIC; that is, $\sqrt{s} = 0.5 - 3\ TeV$ and $L = 500 - 2000\ fb^{-1}$. In addition, in our study we adopt the data reported in Tables 1 and 2, and the relationship between $M_{Z'}$ and g_1' is given by [33, 46, 47]

$$\frac{M_{Z'}}{g_1'} \geq 6.9\ TeV. \quad (22)$$

The constraint given by (22) means that $M_{Z'}$ and g_1' can no longer be considered as independent parameters of the B-L model. Therefore, for our analysis we can only fix one of them. Such a relationship may restrict the search range of the mass of the new boson Z' in the colliders.

In Figure 2, we present the dependence of the $g_{ZZ'h}(\theta', g_1')$ (in GeV units) coupling and $f(\theta', g_1')$, $g(\theta', g_1')$ (see Appendix B) as function of α, and $\theta' = 10^{-3}, 10^{-4}$. From this figure it is clear that $f(\theta', g_1')$ and $g(\theta', g_1')$ are almost α independent, while $g_{ZZ'h}(\theta', g_1')$ is dependent on the scalar mixture angle α.

Figures 3–5 illustrate our results regarding the sensitivity of the Z' heavy gauge boson of the B-L model as a Higgs boson source through the process $e^+e^- \longrightarrow (\gamma, Z, Z') \longrightarrow t\bar{t}h$, including both the resonant and nonresonant effects. In Figure 3, we show the different contributions to the total cross section $\sigma(e^+e^- \longrightarrow t\bar{t}h)$ as a function of the center-of-mass energy $\sqrt{s}$, considering $\theta' = 10^{-3}$ and $g_1' = 0.290$. We see that the cross section corresponding to $\sigma_Z(e^+e^- \longrightarrow t\bar{t}h)$

Table 1: Current experimental data.

Observable	Value	Ref.	Observable	Value	Ref.
$\sin^2\theta_W$	0.23149 ± 0.00016	[35]	m_W	$80.389 \pm 0.023\ GeV$	[35]
m_τ	$1776.82 \pm 0.16\ MeV$	[35]	m_Z	$91.1876 \pm 0.0021\ GeV$	[35]
m_b	$4.6 \pm 0.18\ GeV$	[35]	Γ_Z	$2.4952 \pm 0.0023\ GeV$	[35]
m_t	$172.6 \pm 0.9\ GeV$	[35]	m_h	$125 \pm 0.4\ GeV$	[35]

Table 2: Benchmark model parameters.

$U(1)'$	Mass Z'	Mass H	Mass ν_R	g_1'	θ'	v'	α	Refs.
$U(1)_{B-L}$	$[1-4]\ TeV$	$800\ GeV$	$500\ GeV$	[0-1]	$[10^{-4}, 10^{-3}]$	$3.45\ TeV$	$\pi/9$	[36–40]

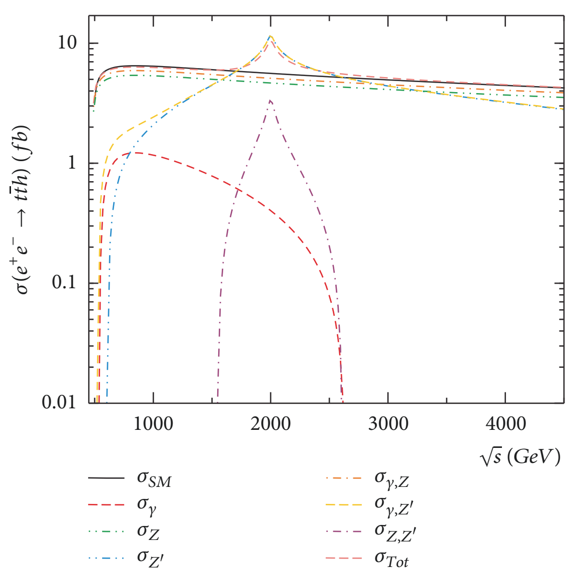

Figure 3: The cross section of the production process $e^+e^- \longrightarrow t\bar{t}h$ as a function of $\sqrt{s}$ for $M_{Z'} = 2000\ GeV$ and $g_1' = 0.290$.

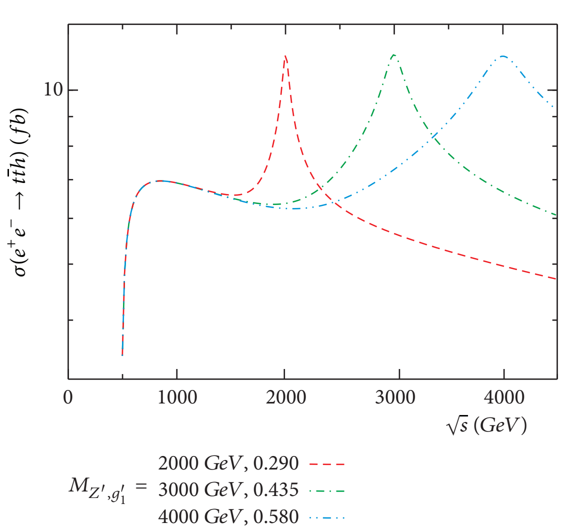

Figure 4: The total cross section of the production process $e^+e^- \longrightarrow t\bar{t}h$ as a function of $\sqrt{s}$. The curves are for $M_{Z'} = 2000\ GeV$ and $g_1' = 0.290$, $M_{Z'} = 3000\ GeV$ and $g_1' = 0.435$, and $M_{Z'} = 4000\ GeV$ and $g_1' = 0.580$, respectively.

decreases for large $\sqrt{s}$. In the case of the cross section of the B-L model (18) and the total cross section (15), respectively, there is an increment for large values of the center-of-mass energy, reaching its maximum value at the resonance Z' heavy gauge boson, which is $\sqrt{s} = 2000\ GeV$.

For the reaction $e^+e^- \longrightarrow t\bar{t}h$, we plot in Figure 4 its associated cross section as a function of the center-of-mass energy $\sqrt{s}$, for heavy gauge boson masses of $M_{Z'} = 2000, 3000, 4000\ GeV$ and $g_1' = 0.290, 0.435, 0.580$, respectively. The choice of the values for $M_{Z'}$ and g_1' is done by keeping the relationship between $M_{Z'}$ and g_1' of (22). Figure 4 shows that the cross section is sensitive to not only the free parameters, but also the height of the resonance peaks for the boson Z', corresponding to the value of $\sqrt{s} = M_{Z'}$. The resonances are broader for larger values of g_1', since the total width of the Z' boson increases with g_1', as shown in Fig. 3 of [13].

Figure 5 describes the correlation between the heavy gauge boson mass $M_{Z'}$ and the g_1' coupling of the $U(1)_{B-L}$ model for the cross section of $\sigma_{Tot} = 7, 8, 9, 10\ fb$ (top panel) with $\sqrt{s} = 2000\ GeV$, $\sigma_{Tot} = 7, 8, 9, 10\ fb$ (central panel) with $\sqrt{s} = 3000\ GeV$, and $\sigma_{Tot} = 7, 8, 9, 10\ fb$ (bottom panel) with $\sqrt{s} = 4000\ GeV$. From there, we see that there is a strong correlation between the gauge boson mass $M_{Z'}$ and the new gauge coupling g_1'.

The sensitivity of the total cross section is evident with respect to the value of the gauge boson mass $M_{Z'}$, center-of-mass energy $\sqrt{s}$, and g_1', which is the new $U(1)_{B-L}$ gauge coupling as shown in Figures 3–5. The total cross section increases with the collider energy, reaching a maximum at the resonance of the Z' gauge boson. In Table 3 we present the $t\bar{t}h$ number of expected events for the center-of-mass energies of $\sqrt{s} = 1000, 2000, 3000\ GeV$, integrated luminosities $\mathscr{L} = 500, 1000, 1500, 2000\ fb^{-1}$, and heavy gauge boson masses $M_{Z'} = 1000, 2000, 3000\ GeV$ with $g_1' = 0.145, 0.290, 0.435$, respectively. The possibility of observing the process $e^+e^- \longrightarrow (\gamma, Z, Z') \longrightarrow t\bar{t}h$ is very promising as shown in Table 3, and it would be possible to perform precision measurements for both the Z' and Higgs boson in the future high-energy and high-luminosity linear e^+e^- colliders experiments. Table 3 also indicates to us that the cross section rises with the energy once the threshold for $t\bar{t}h$ production is reached, until Z' is produced resonantly at $\sqrt{s} = 1000, 2000$ and $3000\ GeV$, respectively. Afterwards it decreases with rising energy due

TABLE 3: Total production of $t\bar{t}h$ in the B-L model for $M_{Z'} = 1000, 2000, 3000\ GeV$, $\mathscr{L} = 500, 1000, 1500, 2000\ fb^{-1}$, $M_h = 125\ GeV$, $\alpha = \pi/9$ and $\theta' = 10^{-3}$.

$\sqrt{s}$ (GeV)	$\mathscr{L} = 500; 1000, 1500; 2000\ fb^{-1}$: $M_{Z'} = 1000\ GeV$, $g_1' = 0.145$	$M_{Z'} = 2000\ GeV$, $g_1' = 0.290$	$M_{Z'} = 3000\ GeV$, $g_1' = 0.435$
1000	5755; 11511; 17266; 23022	2895; 5791; 8687; 11583	1916; 3833; 5750; 7667
2000	11510; 23023; 34531; 46045	5791; 11583; 17374; 23166	3833; 7666; 11500: 15333
300	17265; 34533; 51798; 69067	8668; 17375; 26061; 34749	5749; 11499; 17249; 22999

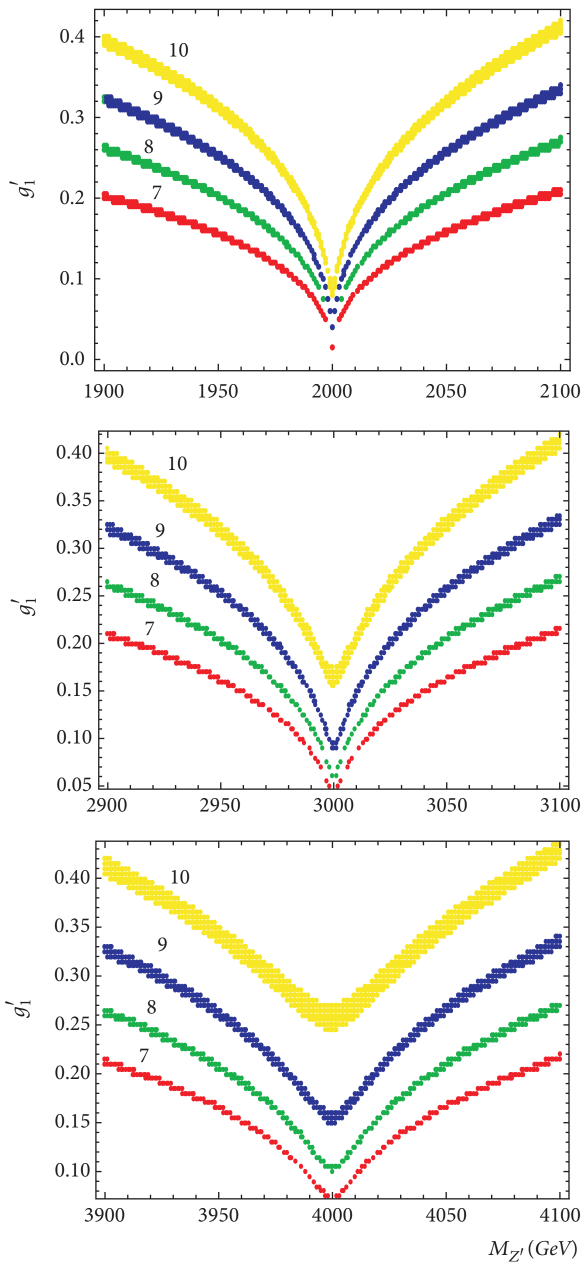

FIGURE 5: Correlation between $M_{Z'}$ and g_1'. Top panel: the contours correspond to $\sigma_{Tot} = 7, 8, 9, 10\,fb$ and $\sqrt{s} = 2000\ GeV$. For the central panel, the contours hold for $\sigma_{Tot} = 7, 8, 9, 10\ fb$ and $\sqrt{s} = 3000\ GeV$ and for the bottom panel $\sigma_{Tot} = 7, 8, 9, 10\ fb$ and $\sqrt{s} = 4000\ GeV$.

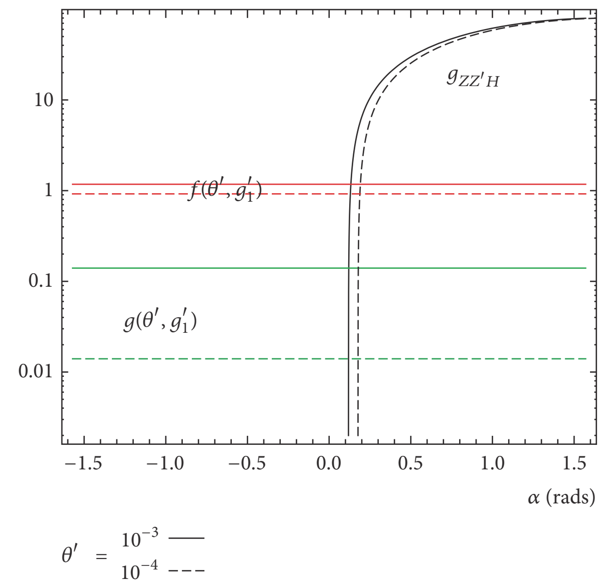

FIGURE 6: Same as in Figure 2, but for $g_{ZZ'H}(\theta', g_1')$, $f(\theta', g_1')$, and $g(\theta', g_1')$.

to the Z and Z' propagators. Another promising production mode for studying the Z' boson and Higgs boson properties of the B-L model is $e^+e^- \longrightarrow (\gamma, Z, Z') \longrightarrow t\bar{t}H$, which is studied next.

We analyze the impact of the parameters of the B-L model on the process $e^+e^- \longrightarrow (\gamma, Z, Z') \longrightarrow t\bar{t}H$. In Figure 6 we present the $g_{ZZ'H}(\theta', g_1')$ (in GeV unit) coupling and $f(\theta', g_1')$, $g(\theta', g_1')$ functions as a function of α, with $\theta' = 10^{-3}, 10^{-4}$. From this figure it is clear that $f(\theta', g_1')$ and $g(\theta', g_1')$ are almost α independent, while $g_{ZZ'H}(\theta', g_1')$ is dependent on the scalar mixing angle α.

The total cross section for the process under study is presented in Figure 7, as a function of the collision energy for $M_h = 125\ GeV$, $M_H = 800\ GeV$, $M_{\nu_R} = 500\ GeV$, $M_{Z'} = 2000\ GeV$, and $g_1' = 0.290\ GeV$. Each curve in figure holds for the different contributions, and they are plotted as a function of the center-of-mass energy $\sqrt{s}$. We can see that the cross section corresponding to $\sigma_Z(e^+e^- \longrightarrow t\bar{t}H)$ decreases for large $\sqrt{s}$. We note again that, for the cross section of the B-L model Eq. (18) and the total cross section Eq. (15), there is an increment for large values of the center-of-mass energy,

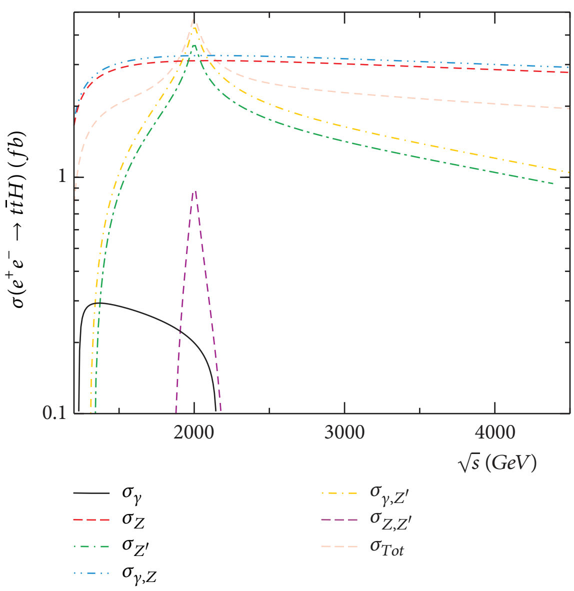

FIGURE 7: Same as in Figure 3, but for $e^+e^- \longrightarrow t\bar{t}H$.

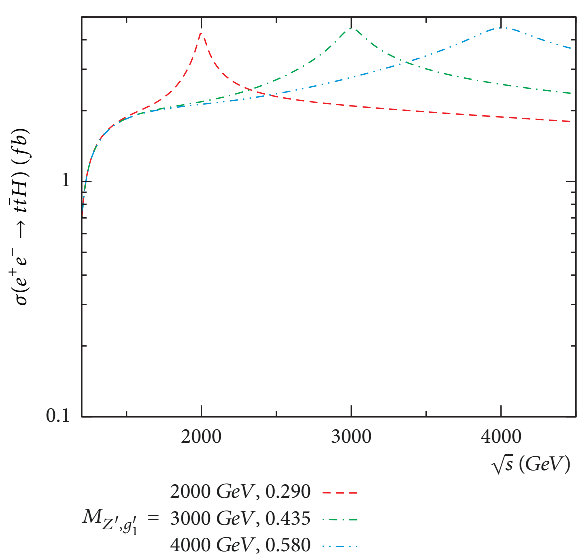

FIGURE 8: Same as in Figure 4, but for $e^+e^- \longrightarrow t\bar{t}H$.

reaching its maximum value at the resonance Z' heavy gauge boson, which is quite near $\sqrt{s} = 2000$ GeV.

We now explore the effects of g_1', $M_{Z'}$ over the total cross section of the process $e^+e^- \longrightarrow t\bar{t}H$ as a function of the center-of-mass energy $\sqrt{s}$. We explore the cases $M_{Z'} = 1000$ GeV with $g_1' = 0.145$, $M_{Z'} = 2000$ GeV with $g_1' = 0.290$, and $M_{Z'} = 3000$ GeV with $g_1' = 0.435$. Our results are plotted in Figure 8. For $\sqrt{s} = M_{Z'}$ the resonant effect dominates and the cross section is sensitive to the free parameters.

In Figure 9, we show the correlation between the boson mass $M_{Z'}$ and the g_1' coupling for the cross section values of $\sigma_{Tot} = 1, 2, 3, 4$ fb (top panel), $\sigma_{Tot} = 1, 2, 3, 4$ fb (central

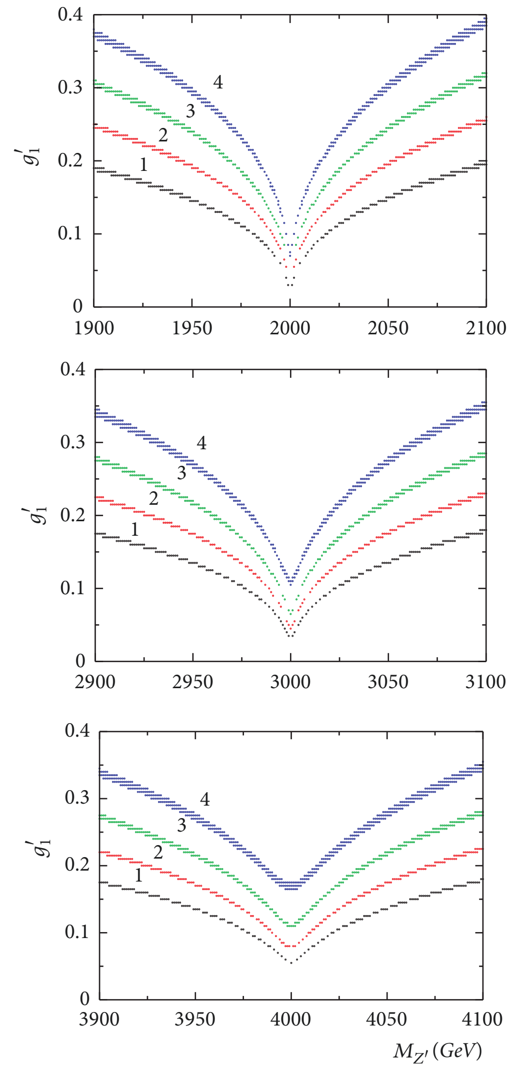

FIGURE 9: Same as in Figure 5, but for $e^+e^- \longrightarrow t\bar{t}H$.

panel), and $\sigma_{Top} = 1, 2, 3, 4$ fb (bottom panel). The plots expose a strong correlation between $M_{Z'}$ and g_1'.

Altogether, Figures 6–9 clearly show how sensitive the total cross section is, to the value of the boson mass $M_{Z'}$, to center-of-mass energy $\sqrt{s}$ and g_1', and how it increments with the collider energy reaching a maximum at the resonance of the Z' gauge boson. The $t\bar{t}H$ number of events which are expected to be observed are shown in Table 4; these were obtained for center-of-mass energies of $\sqrt{s} = 1000, 2000, 3000$ GeV, integrated luminosity $\mathscr{L} = 500, 1000, 1500, 2000$ fb^{-1}, and heavy gauge boson masses of $M_{Z'} = 1000, 2000, 3000$ GeV with $g_1' = 0.145, 0.290, 0.435$, respectively. These numbers encourage the possibility of observing the process $e^+e^- \longrightarrow (\gamma, Z, Z') \longrightarrow t\bar{t}H$. We observe from Table 4 that the cross section grows with the energy once the threshold for $t\bar{t}H$ production is reached, until the Z' is produced resonantly at $\sqrt{s} = 1000, 2000$ and 3000 GeV.

Table 4: Total production of $t\bar{t}H$ in the B-L model for $M_{Z'} = 1000, 2000, 3000\ GeV$, $\mathscr{L} = 500, 1000, 1500, 2000\ fb^{-1}$, $M_H = 800\ GeV$, $\alpha = \pi/9$ and $\theta' = 10^{-3}$.

	$\mathscr{L} = 500; 1000; 1500; 2000\ fb^{-1}$		
$\sqrt{s}\ (GeV)$	$M_{Z'} = 1000\ GeV$ $g_1' = 0.145$	$M_{Z'} = 2000\ GeV$ $g_1' = 0.290$	$M_{Z'} = 3000\ GeV$ $g_1' = 0.435$
1000	4381; 8763; 13144; 17526	1629; 3259; 4887; 6518	748; 1497; 2246; 2994
2000	8762; 17527; 26288; 35052	3258; 6517; 9775; 13034	1496; 2995; 4491; 5989
3000	13143; 26289; 39432; 52578	4886; 9776; 14663; 19551	2245; 4491; 6736; 8982

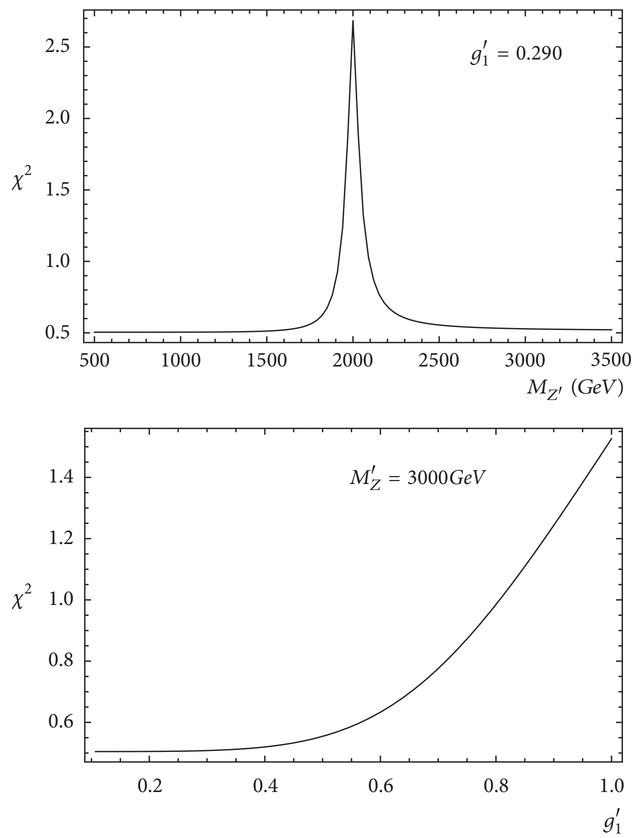

Figure 10: χ^2 as a function of $M_{Z'}$ (g_1').

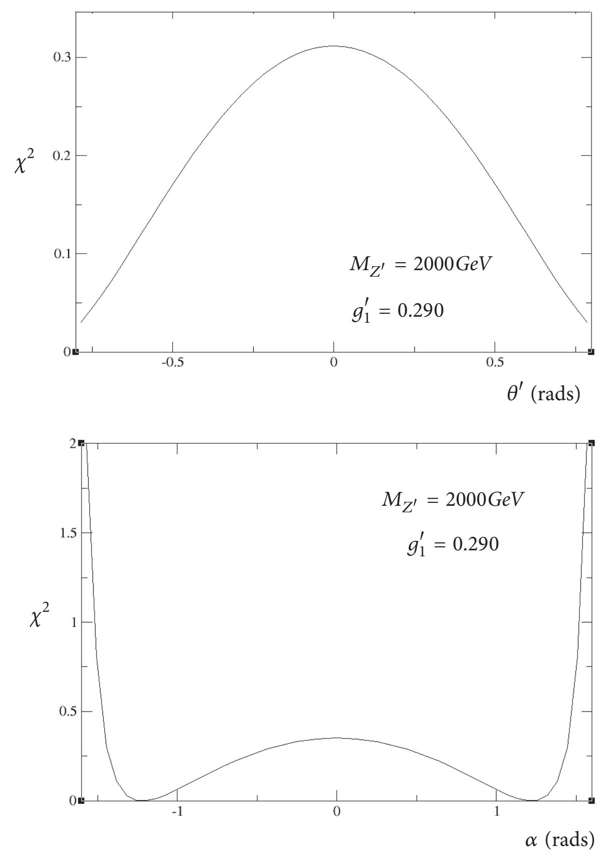

Figure 11: χ^2 as a function of θ' (α).

Afterwards it decreases with rising energy due to the Z and Z' propagators.

Finally, to investigate the sensitivity to the parameters of the B-L model in $e^+e^- \longrightarrow t\bar{t}h$ process we use the chi-squared function. The χ^2 function is defined as follows [48–54]:

$$\chi^2 = \left(\frac{\sigma_{SM} - \sigma_{B-L}}{\sigma_{SM}\delta}\right)^2, \tag{23}$$

where σ_{B-L} is the total cross section including contributions from the SM and new physics, $\delta = \sqrt{(\delta_{st})^2 + (\delta_{sys})^2}$, $\delta_{st} = 1/\sqrt{N_{SM}}$ is the statistical error, and δ_{sys} is the systematic error. The number of events is given by $N_{SM} = \mathscr{L}_{int} \times \sigma_{SM}$, where $\mathscr{L}_{int}$ is the integrated CLIC luminosity.

In Figures 10 and 11, we plot the χ^2 distribution as a function of $M_{Z'}$ (g_1', θ', α). We plot the curves for each case, for which we have divided the $M_{Z'}(g_1', \theta', \alpha)$ interval into several bins.

The most important systematic errors are due to the modelling of the signal and the background. For our analysis we choose a systematic error of $\delta_{sys} = 10\%$ [1, 3, 55, 56], which is a reasonably moderate value. This value was chosen considering that the tth cross section can be measured with an accuracy of 12% in the semileptonic channel and 11% in the hadronic channel. The combined precision of the two channels is 8% [1, 3, 55, 56]. Furthermore, the machine-related uncertainties, such as the knowledge of the center-of-mass energy of the collider and the luminosity, are also relevant for this study. We can assumed that the CLIC will be built in the coming years and the systematic uncertainties will be lower when considering the development of future detector technology.

It must be noted that the sensitivity for the parameters of the B-L model, $M_{Z'}$, g_1', θ', and α, is good as is shown in Figures 10 and 11. However, it is worth mentioning that it is necessary to carry out a complete and detailed study on the sensitivity of the aforementioned parameters; for this, kinematic cuts must be applied on the particles of the final state to reduce the background and to optimize the signal sensitivity.

Future electron-positron linear colliders operating as Higgs factories, and having the advantages of a clean collider environment and large statistics, could greatly enhance the sensitivity to study in detail the production and decay processes of various particles. In addition, the sensitivity increases by increasing the center-of-mass energy and the integrated luminosity. Furthermore, if we consider the cleanest modes and new models beyond the SM, large cross sections and little background from the SM, combined with the high luminosity of the colliders, result in large data samples allowing precise measurements with high sensitivity.

The presented results definitely are inside the scope of detection in future experiment with improved sensitivity of the next generation of linear colliders. The processes $e^+e^- \longrightarrow t\bar{t}h, t\bar{t}H$ will be an important tool for the precision measurements of the top Yukawa coupling and to study some, or all, the implications of the CP violation Higgs-top coupling [57]. As an application of this process, another point to study is the importance of the Higgs-top coupling in the hierarchy problem [58] and a deeper understanding of the vacuum stability of the SM [59, 60]. In this regard, we study the CP violation Higgs-top coupling in the context of the B-L model at future e^+e^- colliders energies [61].

Once we have extensively studied the production of light and heavy Higgs boson in the context of extension $U(1)_{B-L}$ of the SM, with an additional Z' boson, we can conclude that our results seem to be achievable with the capability of future linear colliders (ILC and CLIC) with center-of-mass energies of $\sqrt{s} = 500-3000\ GeV$ and integrated luminosities of $\mathscr{L} = 500 - 2000\ fb^{-1}$. Our study covered the processes $e^+e^- \longrightarrow (\gamma, Z, Z') \longrightarrow t\bar{t}h$ and $e^+e^- \longrightarrow (\gamma, Z, Z') \longrightarrow t\bar{t}H$, including resonant and nonresonant effects. We find that the total number of expected $t\bar{t}h$ and $t\bar{t}H$ events can reach 69,067 and 52,578, respectively. Under this optimistic scenario it would be possible to perform precision measurements for both Higgs bosons h and H, for the Z' heavy gauge boson, and for the full parameters of the models θ', g_1', and α. The SM expression for the cross section of the reaction $e^+e^- \longrightarrow t\bar{t}h$ can be recovered in the decoupling limit, when $\theta' = 0$, $g_1' = 0$, and $\alpha = 0$. In this case, the terms depending on θ', g_1', and α in (15) are zero and therefore (15) reduces to the SM case [41–45]. Our study complements other studies on the $U(1)_{B-L}$ model and on the single Higgs bosons production processes $e^+e^- \longrightarrow t\bar{t}h$ and $e^+e^- \longrightarrow t\bar{t}H$, which seems to be suitable for experiments at hadron and e^+e^- colliders.

Appendix

A. Formulas for $\Gamma_i(g_V'^f, g_A'^f, x_1, x_2)$ and $\Gamma_i(x_1, x_2)$

In this appendix the explicit formulas for $\Gamma_i(g_V'^f, g_A'^f, x_1, x_2)$ and $\Gamma_i(x_1, x_2)$, $i = 1, 2, \ldots, 6$ corresponding to the decay widths of the reactions $\Gamma(Z' \longrightarrow f\bar{f}h, f\bar{f}H)$ and $\Gamma(Z' \longrightarrow W^+W^-h, W^+W^-H)$ are given by

$$\Gamma_1\left(g_V'^f, g_A'^f, x_1, x_2\right) = \int_{x_1^-}^{x_1^+}\int_{x_2^-}^{x_2^+} G_F m_f^2\left(\cos^2\alpha, \sin^2\alpha\right) \times \left[-\frac{2}{\left(x_1 - x_2 - 1\right)^2}\left\{\left(g_V'^f\right)^2\left(-16\frac{m_f^4}{M_{Z'}^4}\right.\right.\right.$$

$$+ 4\frac{m_f^2}{M_{Z'}^2}\left(\frac{m_{h,H}^2}{M_{Z'}^2} + x_1^2 + 2x_1\left(x_2 - 2\right) + \left(x_2 - 4\right)x_2 + 1\right)$$

$$\left.+ \left(x_1 + x_2\right)\left(-\frac{m_{h,H}^2}{M_{Z'}^2}\left(x_1 + x_2 - 2\right) + x_1\left(x_1 + x_2 - 3\right) + x_2\right) + \frac{m_{h,H}^2}{M_{Z'}^2} + x_1 - 2x_2 + 1\right) + \left(g_A'^f\right)^2\left(32\frac{m_f^4}{M_{Z'}^4}\right.$$

$$+ 4\frac{m_f^2}{M_{Z'}^2}\left(-2\frac{m_f^2}{M_{Z'}^2} + x_1^2 + 2x_1\left(x_2 + 1\right) + x_2\left(x_2 + 2\right) - 5\right)$$

$$\left.\left.+ \left(x_1 + x_2\right)\left(-\frac{m_{h,H}^2}{M_{Z'}^2}\left(x_1 + x_2 - 2\right) + x_1\left(x_1 + x_2 - 3\right) + x_2\right) + \frac{m_{h,H}^2}{M_{Z'}^2} + x_1 - 2x_2 + 1\right)\right\} + \frac{2}{\left(x_2 - 1\right)^2}\left\{\left(g_V'^f\right)^2\right.$$

$$\cdot\left(-\frac{m_{h,H}^2}{M_{Z'}^2}\left(8\frac{m_f^2}{M_{Z'}^2} + \left(x_2 - 2\right)x_2 - 1\right) - \left(x_2 - 1\right)\left(x_1x_2 + x_1 + x_2 - 1\right)\right) - \left(g_A'^f\right)^2$$

$$\left.\cdot\left(\frac{m_{h,H}^2}{M_{Z'}^2}\left(4\frac{m_f^2}{M_{Z'}^2} - \left(x_2 - 2\right)x_2 + 1\right) + \left(x_2 - 1\right)\left(x_1x_2 + x_1 + x_2 - 1\right)\right)\right\} + \frac{4}{\left(x_1 - x_2 - 1\right)\left(x_2 - 1\right)}\left\{\left(g_V'^f\right)^2\right.$$

$$\cdot\left(2\frac{m_f^2}{M_{Z'}^2}\left(4\frac{m_{h,H}^2}{M_{Z'}^2} + \left(x_1 + 4\right)x_2 + x_1 - 4\right) - 2\frac{m_{h,H}^4}{M_{Z'}^4} - \frac{m_{h,H}^2}{M_{Z'}^2}\left(x_1\left(x_2 - 3\right) + \left(x_2 - 1\right)^2\right)\right.$$

$$+\left(x_1+1\right)\left(x_2-1\right)\left(x_1-x_2-1\right)\Big)+\left(g_A^{\prime f}\right)^2\left(2\frac{m_f^2}{M_{Z'}^2}\left(-4\frac{m_{h,H}^2}{M_{Z'}^2}+x_1^2+\left(x_1-2\right)x_2+x_1\right)+2\frac{m_{h,H}^4}{M_{Z'}^4}\right.$$

$$\left.+\frac{m_{h,H}^2}{M_{Z'}^2}\left(x_1\left(x_2-3\right)+\left(x_2-1\right)^2-\left(x_1+1\right)\left(x_2-1\right)\left(x_1+x_2-1\right)\right)\right)\Big\}\Big]dx_1dx_2, \quad \text{(A.1)}$$

$$\Gamma_2\left(g_V^{\prime f},g_A^{\prime f},x_1,x_2\right)=\int_{x_1^-}^{x_1^+}\int_{x_2^-}^{x_2^+}\frac{2M_W^2M_{Z'}^2}{\left(-m_{h,H}^2+m_Z^2+M_{Z'}^2x_1-M_{Z'}^2\right)^2}\times\Big[\left(g_V^{\prime f}\right)^2\Big(4\frac{m_f^2}{M_{Z'}^2}+\frac{m_{h,H}^2}{M_{Z'}^2}-x_1x_2-x_1-x_2^2+2x_2$$

$$+1\Big)-\left(g_A^{\prime f}\right)^2\left(8\frac{m_f^2}{M_{Z'}^2}-\frac{m_{h,H}^2}{M_{Z'}^2}+\left(x_1-2\right)x_2+x_1+x_2^2-1\right)\Big]\times\left[f\left(\theta',g_1'\right)\cos\alpha\mp g\left(\theta',g_1'\right)\sin\alpha\right]^2dx_1dx_2, \quad \text{(A.2)}$$

$$\Gamma_3\left(g_V^{\prime f},g_A^{\prime f},x_1,x_2\right)=\int_{x_1^-}^{x_1^+}\int_{x_2^-}^{x_2^+}\left(\frac{m_f}{v}\right)(\cos\alpha,\sin\alpha)\times\Big[\frac{2m_fM_W}{\left(x_1+x_2-1\right)\left(-m_{h,H}^2+M_Z^2+M_{Z'}^2x_1+M_{Z'}^2\right)}\times\Big\{\left(g_V^fg_V^{\prime f}\right)$$

$$\cdot\left(2\frac{m_{h,H}^2}{M_{Z'}^2}-8\frac{m_f^2}{M_{Z'}^2}+\left(x_1+x_2-3\right)\left(x_1+2x_2\right)\right)+\left(g_A^fg_A^{\prime f}\right)\Big(16\frac{m_f^2}{M_{Z'}^2}-4\frac{m_{h,H}^2}{M_{Z'}^2}+x_1\left(x_1+3\right)+3x_1x_2+2x_2^2 \quad \text{(A.3)}$$

$$-6\Big)\Big\}\Big]\times\left[f\left(\theta',g_1'\right)\cos\alpha\mp g\left(\theta',g_1'\right)\sin\alpha\right]dx_1dx_2,$$

where the limits of integration are

$$\frac{2m_f}{M_{Z'}}\le x_1\le 1-\frac{m_{h,H}^2}{M_{Z'}^2}-\frac{2m_fm_{h,H}}{M_{Z'}^2},$$

$$x_2=\pm\left(x_1^2-4\frac{m_f^2}{M_{Z'}^2}\right)^{1/2}\left[\left(1+\frac{m_f^2}{M_{Z'}^2}-x_1\right)^2+\frac{m_f^4}{M_{Z'}^4}+\frac{m_{h,H}^4}{M_{Z'}^4}-2\left(1+\frac{m_f^2}{M_{Z'}^2}-x_1\right)\left(\frac{m_f^2}{M_{Z'}^2}\right)-2\left(1+\frac{m_f^2}{M_{Z'}^2}-x_1\right)\left(\frac{m_{h,H}^2}{M_{Z'}^2}\right)-2\left(\frac{m_f^2}{M_{Z'}^2}\right)\left(\frac{m_{h,H}^2}{M_{Z'}^2}\right)\right]^{1/2}. \quad \text{(A.4)}$$

$\Gamma_i(x_1,x_2)$ for the decay widths at three bodies involving vector bosons W^+W^- are

$$\Gamma_4\left(x_1,x_2\right)=\int_{x_1^-}^{x_1^+}\int_{x_2^-}^{x_2^+}\frac{1}{4\left(x_1+x_2-1\right)^2}\times\Big[4\left(x_1-x_2-14\right)\left(\frac{M_W^6}{M_{Z'}^6}\right)$$

$$+4\left(3x_2^2+6x_1x_2-20x_2+2\left(x_1-5\right)x_1+17\right)\left(\frac{M_W^4}{M_{Z'}^4}\right)$$

$$+\left(x_1^3+\left(3x_2-2\right)x_1^2+\left(x_2-1\right)\left(7x_2-3\right)x_1+\left(x_2-1\right)^2\left(5x_2-14\right)\right)\left(\frac{M_W^2}{M_{Z'}^2}\right)+\left(x_1-x_2+1\right)\left(x_2-1\right)^2 \quad \text{(A.5)}$$

$$-\left(\frac{m_{h,H}^4}{M_{Z'}^4}\right)\left(x_2-x_1^2+x_1+\frac{M_W^2}{M_{Z'}^2}\left(x_1-x_2+2\right)-1\right)$$

$$+2\left(\frac{m_{h,H}^2}{M_{Z'}^2}\right)\left(8\frac{M_W^4}{M_{Z'}^4}-\left(x_2^2+3x_1x_2-7x_2+x_1\left(2x_1-7\right)+6\right)\left(\frac{M_W^2}{M_{Z'}^2}\right)-\left(x_2-1\right)^2\right)\Big]dx_1dx_2,$$

$$\Gamma_5(x_1,x_2)=\int_{x_1^-}^{x_1^+}\int_{x_2^-}^{x_2^+}\frac{1}{16(x_2-1)^2}\left[8\left(\frac{m_{h,H}^6}{M_{Z'}^6}\right)\right.$$
$$+\left(x_1^2+4(2x_2-3)x_1+16(x_2-1)^2+\left(\frac{M_W^2}{M_{Z'}^2}\right)\left(-8x_1^2+8x_2-52\right)\right)\left(\frac{m_{h,H}^4}{M_{Z'}^4}\right)$$
$$+2\left(8(x_1-x_2+7)\left(\frac{M_W^4}{M_{Z'}^4}\right)-4(x_2-1)(3x_1-6x_2-7)\left(\frac{M_W^2}{M_{Z'}^2}\right)\right)-\left(x_1^2+4(x_2-1)x_1+4(x_2-1)^2\right)\left(\frac{m_{h,H}^2}{M_{Z'}^2}\right) \quad \text{(A.6)}$$
$$+x_1(x_1+4)(x_2-1)^2+16\left(\frac{M_W^6}{M_{Z'}^6}\right)(x_1-x_2-14)-8\left(\frac{M_W^4}{M_{Z'}^4}\right)\left(x_1^2-4x_1-8x_2^2+14x_2-16\right)$$
$$\left.+4\left(\frac{M_W^2}{M_{Z'}^2}\right)\left((2x_2-1)x_1^2+4(x_2-1)x_1x_2+(x_2-1)^2(2x_2-1)\right)\right]dx_1dx_2,$$

$$\Gamma_6(x_1,x_2)=\int_{x_1^-}^{x_1^+}\int_{x_2^-}^{x_2^+}\frac{M_{Z'}^2}{8\left(-2m_{h,H}^2+2M_W^2+x_2M_{Z'}^2-M_{Z'}^2\right)(x_1+x_2-1)}\times\left[\left(\frac{m_{h,H}^6}{M_{Z'}^6}\right)\right.$$
$$+\left(\left(\frac{M_W^4}{M_{Z'}^4}\right)+4x_1x_2+2\left(\frac{M_W^2}{M_{Z'}^2}\right)(x_1-x_2-8)+3(1-2x_1-x_2)\right)\left(\frac{M_W^4}{M_{Z'}^4}\right)+\left(4(x_2-x_1+22)\frac{M_W^4}{M_{Z'}^4}\right)$$
$$-\left(5x_1^2+16x_1x_2-24x_1+12x_2^2-40x_2+28\right)\left(\frac{M_W^2}{M_{Z'}^4}\right)-(x_2-1)\left(x_1^2+5x_2-5\right)\left(\frac{m_{h,H}^2}{M_{Z'}^2}\right) \quad \text{(A.7)}$$
$$+(2x_1-x_2+1)(x_2-1)^2+8\left(\frac{M_W^6}{M_{Z'}^6}\right)(x_1-x_2-14)+4\left(\frac{M_W^4}{M_{Z'}^4}\right)\left(7x_2^2-27x_2+x_1(6x_2-8)+20\right)$$
$$\left.+\left(\frac{M_W^2}{M_{Z'}^2}\right)\left(x_1^3+(5x_2-3)x_1^2+\left(6x_2^2-4x_2-2\right)x_1+6(x_2-2)\right)\right]dx_1dx_2,$$

where the limits of integration are

$$\frac{2M_W}{M_{Z'}}\le x_1\le 1-\frac{m_{h,H}^2}{M_{Z'}^2}-\frac{2M_Wm_{h,H}}{M_{Z'}^2},$$
$$x_2=\pm\left(x_1^2-4\frac{M_W^2}{M_{Z'}^2}\right)^{1/2}\left[\left(1+\frac{M_W^2}{M_{Z'}^2}-x_1\right)^2+\frac{M_W^4}{M_{Z'}^4}\right. \quad \text{(A.1)}$$
$$+\frac{m_{h,H}^4}{M_{Z'}^4}-2\left(1+\frac{M_W^2}{M_{Z'}^2}-x_1\right)\left(\frac{M_W^2}{M_{Z'}^2}\right)$$
$$-2\left(1+\frac{M_W^2}{M_{Z'}^2}-x_1\right)\left(\frac{m_{h,H}^2}{M_{Z'}^2}\right)$$
$$\left.-2\left(\frac{M_W^2}{M_{Z'}^2}\right)\left(\frac{m_{h,H}^2}{M_{Z'}^2}\right)\right]^{1/2}. \quad \text{(A.8)}$$

B. Transition Amplitudes and Formulas for $I_i(x_1,x_2)$

We present the transition amplitudes for the processes $e^+e^-\longrightarrow(\gamma,Z,Z')\longrightarrow t\bar{t}h,t\bar{t}H$, as well as the formulas for $I_i(x_1,x_2)$:

$$\mathcal{M}_1=\frac{-ie^2m_t(\cos\alpha,\sin\alpha)}{v\left(l^2-m_t^2\right)}\left[\bar{u}(p_3)(\not{l}+m_t)\gamma^\alpha v(p_4)\right]\frac{g_{\alpha\beta}}{\left[(p_1+p_2)^2\right]}\left[\bar{u}(p_2)\gamma^\beta v(p_1)\right], \quad \text{(B.1)}$$

$$\mathcal{M}_2=\frac{-ie^2m_t(\cos\alpha,\sin\alpha)}{v\left(l'^2-m_t^2\right)}\left[\bar{u}(p_3)\gamma^\alpha\left(\not{l}'+m_t\right)v(p_4)\right]\frac{g_{\alpha\beta}}{\left[(p_1+p_2)^2\right]}\left[\bar{u}(p_2)\gamma^\beta v(p_1)\right], \quad \text{(B.2)}$$

$$\begin{aligned}\mathscr{M}_3 = {} & \frac{-ig^2 m_t (\cos\alpha, \sin\alpha)}{4v\cos^2\theta_W (k^2 - m_t^2)} \left[\overline{u}(p_3)(\not{k} + m_t)\gamma^\alpha \left(g_V^t - g_A^t \gamma_5\right) v(p_4)\right] \\ & \times \frac{\left(g_{\alpha\beta} - p_\alpha p_\beta / M_Z^2\right)}{\left[(p_1 + p_2)^2 - M_Z^2 - iM_Z\Gamma_Z\right]} \left[\overline{u}(p_2)\gamma^\beta \left(g_V^e - g_A^e\gamma_5\right) v(p_1)\right],\end{aligned} \tag{B.3}$$

$$\begin{aligned}\mathscr{M}_4 = {} & \frac{-ig^2 m_t (\cos\alpha, \sin\alpha)}{4v\cos^2\theta_W (k'^2 - m_t^2)} \left[\overline{u}(p_3)\gamma^\alpha \left(g_V^t - g_A^t \gamma_5\right)\left(\not{k}' + m_t\right) v(p_4)\right] \\ & \times \frac{\left(g_{\alpha\beta} - p_\alpha p_\beta / M_Z^2\right)}{\left[(p_1 + p_2)^2 - M_Z^2 - iM_Z\Gamma_Z\right]} \left[\overline{u}(p_2)\gamma^\beta \left(g_V^e - g_A^e\gamma_5\right) v(p_1)\right],\end{aligned} \tag{B.4}$$

$$\begin{aligned}\mathscr{M}_5 = {} & \frac{-ig^2 m_t (\cos\alpha, \sin\alpha)}{4v\cos^2\theta_W (r^2 - m_t^2)} \left[\overline{u}(p_3)(\not{r} + m_t)\gamma^\alpha \left(g_V^{\prime t} - g_A^{\prime t} \gamma_5\right) v(p_4)\right] \\ & \times \frac{\left(g_{\alpha\beta} - p_\alpha p_\beta / M_{Z'}^2\right)}{\left[(p_1 + p_2)^2 - M_{Z'}^2 - iM_{Z'}\Gamma_{Z'}\right]} \left[\overline{u}(p_2)\gamma^\beta \left(g_V^{\prime e} - g_A^{\prime e}\gamma_5\right) v(p_1)\right],\end{aligned} \tag{B.5}$$

$$\begin{aligned}\mathscr{M}_6 = {} & \frac{-ig^2 m_t (\cos\alpha, \sin\alpha)}{4v\cos^2\theta_W (r'^2 - m_t^2)} \left[\overline{u}(p_3)\gamma^\alpha \left(g_V^{\prime t} - g_A^{\prime t} \gamma_5\right)\left(\not{r}' + m_t\right) v(p_4)\right] \\ & \times \frac{\left(g_{\alpha\beta} - p_\alpha p_\beta / M_{Z'}^2\right)}{\left[(p_1 + p_2)^2 - M_{Z'}^2 - iM_{Z'}\Gamma_{Z'}\right]} \left[\overline{u}(p_2)\gamma^\beta \left(g_V^{\prime e} - g_A^{\prime e}\gamma_5\right) v(p_1)\right],\end{aligned} \tag{B.6}$$

$$\begin{aligned}\mathscr{M}_7 = {} & \frac{ig^2 m_Z^2 (\cos\alpha, \sin\alpha)}{2v\cos^2\theta_W} \left[\overline{u}(p_3)\gamma^\alpha \left(g_V^t - g_A^t \gamma_5\right) v(p_4)\right] \\ & \times \frac{\left(g_{\alpha\beta} - p_\alpha p_\beta / M_Z^2\right)}{\left[(p_1 + p_2)^2 - M_Z^2 - iM_Z\Gamma_Z\right]\left[(p_3 + p_4)^2 - M_Z^2 - iM_Z\Gamma_Z\right]} \times \left[\overline{u}(p_2)\gamma^\beta \left(g_V^e - g_A^e\gamma_5\right) v(p_1)\right],\end{aligned} \tag{B.7}$$

$$\begin{aligned}\mathscr{M}_8 = {} & \frac{-ig^2 m_Z^2}{2v\cos^2\theta_W} \left[\overline{u}(p_3)\gamma^\alpha \left(g_V^{\prime t} - g_A^{\prime t} \gamma_5\right) v(p_4)\right] \times \frac{\left(g_{\alpha\beta} - p_\alpha p_\beta / M_Z^2 - p_\alpha p_\beta / M_{Z'}^2 + p_\alpha p_\beta / \left(M_Z M_{Z'}\right)\right)}{\left[(p_1 + p_2)^2 - M_Z^2 - iM_Z\Gamma_Z\right]\left[(p_3 + p_4)^2 - M_{Z'}^2 - iM_{Z'}\Gamma_{Z'}\right]} \\ & \times \left[\overline{u}(p_2)\gamma^\beta \left(g_V^e - g_A^e\gamma_5\right) v(p_1)\right]\left[f\left(\theta', g_1'\right)\cos\alpha \mp g\left(\theta', g_1'\right)\sin\alpha\right],\end{aligned} \tag{B.8}$$

$$\begin{aligned}\mathscr{M}_9 = {} & \frac{-ig^2 m_Z^2}{2v\cos^2\theta_W} \left[\overline{u}(p_3)\gamma^\alpha \left(g_V^t - g_A^t \gamma_5\right) v(p_4)\right] \times \frac{\left(g_{\alpha\beta} - p_\alpha p_\beta / M_{Z'}^2 - p_\alpha p_\beta / M_Z^2 + p_\alpha p_\beta / \left(M_Z M_{Z'}\right)\right)}{\left[(p_1 + p_2)^2 - M_{Z'}^2 - iM_{Z'}\Gamma_{Z'}\right]\left[(p_3 + p_4)^2 - M_Z^2 - iM_Z\Gamma_Z\right]} \\ & \times \left[\overline{u}(p_2)\gamma^\beta \left(g_V^{\prime e} - g_A^{\prime e}\gamma_5\right) v(p_1)\right]\left[f\left(\theta', g_1'\right)\cos\alpha \mp g\left(\theta', g_1'\right)\sin\alpha\right],\end{aligned} \tag{B.9}$$

$$\begin{aligned}\mathscr{M}_{10} = {} & \frac{i4g^2 g_1^{\prime 2} v' (\sin\alpha, \cos\alpha)}{\cos^2\theta_W} \left[\overline{u}(p_3)\gamma^\alpha \left(g_V^{\prime t} - g_A^{\prime t} \gamma_5\right) v(p_4)\right] \\ & \times \frac{\left(g_{\alpha\beta} - p_\alpha p_\beta / M_{Z'}^2\right)}{\left[(p_1 + p_2)^2 - M_{Z'}^2 - iM_{Z'}\Gamma_{Z'}\right]\left[(p_3 + p_4)^2 - M_{Z'}^2 - iM_{Z'}\Gamma_{Z'}\right]} \times \left[\overline{u}(p_2)\gamma^\beta \left(g_V^{\prime e} - g_A^{\prime e}\gamma_5\right) v(p_1)\right].\end{aligned} \tag{B.10}$$

In these equations, $p_1, p_2(p_3, p_4)$ stands for the momentum of the positron, electron (top, antitop). $l, k, r(l', k', r')$ stands for the momentum of the virtual top (antitop) (see Feynman diagrams 1, 3, and 5 (2, 4, and 6)). The coupling constants $g_V^e(g_V^t)$, $g_A^e(g_A^t)$, $g_V^{\prime e}(g_V^{\prime t})$, and $g_A^{\prime e}(g_A^{\prime t})$ and $\Gamma(Z')$ for the two body processes are given in [13, 14], while $\Gamma(Z')$ at three bodies are given in (13) and (14). The couplings $g_{ZZ'h}(g_{ZZ'H})$ and the functions $f(\theta', g_1')$ and $g(\theta', g_1')$ are defined as

$$g_{ZZ'h} = 2\left[\frac{1}{4}v\cos\alpha f\left(\theta', g_1'\right) - v'\sin\alpha g\left(\theta', g_1'\right)\right], \tag{B.11}$$

$$g_{ZZ'H} = 2\left[\frac{1}{4}v\sin\alpha f\left(\theta', g_1'\right) + v'\cos\alpha g\left(\theta', g_1'\right)\right], \tag{B.12}$$

$$f\left(\theta', g_1'\right) = \left(\frac{4M_Z^2}{v^2} - g_1'^2\right)\sin\left(2\theta'\right) + \left(\frac{4g_1'M_Z}{v}\right)\cos\left(2\theta'\right), \tag{B.13}$$

$$g\left(\theta', g_1'\right) = 4g_1'^2\left(\frac{v'}{v}\right)\sin\left(2\theta'\right). \tag{B.14}$$

The explicit formulas for the integrants $I_i(x_1, x_2)$, $i = 1, 2, \ldots, 10$ corresponding to the cross section of the processes $e^+e^- \longrightarrow (\gamma, Z, Z') \longrightarrow t\bar{t}h, t\bar{t}H$ are given by

$$\begin{aligned} I_1\left(x_1, x_2\right) = {} & \frac{m_t^2\left(\cos^2\alpha, \sin^2\alpha\right)}{4\pi v^2\left(1-x_1\right)\left(1-x_2\right)}\left[\left(2-x_1-x_2\right)^2 - \frac{m_{h,H}^2}{s}\left(\frac{\left(2-x_1-x_2\right)^2}{\left(1-x_1\right)\left(1-x_2\right)} + 2\left(1-x_1-x_2-\frac{m_{h,H}^2}{s}\right)\right)\right. \\ & \left. + \frac{2m_t^2}{s}\left(4\left(2-x_1-x_2-\frac{m_{h,H}^2}{s}\right) + \frac{\left(2-x_1-x_2\right)^2}{\left(1-x_1\right)\left(1-x_2\right)}\left(\frac{4m_t^2}{s} - \frac{m_{h,H}^2}{s} + 2\right)\right)\right], \end{aligned} \tag{B.15}$$

$$\begin{aligned} I_2\left(x_1, x_2\right) = {} & \frac{m_t^2\left(\cos^2\alpha, \sin^2\alpha\right)}{2\pi v^2\left(1-x_1\right)\left(1-x_2\right)}\left[\left(1-x_1\right)\left(1-x_2\right)\left(3-x_1-x_2\right)\right. \\ & - \frac{m_{h,H}^2}{s}\left(\left(1-x_1\right)\left(1-x_2\right) + \frac{8m_t^2}{s} + 2\left(2-x_1-x_2\right) - \frac{2m_{h,H}^2}{s}\right) \\ & \left. + \frac{3m_t^2}{s}\left(2-x_1-x_2\right)\left(\frac{\left(2-x_1-x_2\right)}{3} + 4 + \frac{\left(2-x_1-x_2\right)}{\left(1-x_1\right)\left(1-x_2\right)}\left(\frac{4m_t^2}{s} - \frac{m_{h,H}^2}{s}\right)\right)\right], \end{aligned} \tag{B.16}$$

$$\begin{aligned} I_3\left(x_1, x_2\right) = {} & \frac{2M_Z^2\left(\cos^2\alpha, \sin^2\alpha\right)}{\pi v^2\left(1-x_1-x_2-m_{h,H}^2/s+M_Z^2/s\right)^2}\left[\frac{m_t^2}{s}\left(\frac{4m_{h,H}^2}{s} - \left(2-x_1-x_2\right)^2 - \frac{12M_Z^2}{s}\right)\right. \\ & \left. + \frac{m_t^2}{M_Z^2}\left(\frac{4m_{h,H}^2}{s} - \left(2-x_1-x_2\right)^2\right)\left(1-x_1-x_2-\frac{m_{h,H}^2}{s} + \frac{M_Z^2}{s}\right)\right], \end{aligned} \tag{B.17}$$

$$I_4\left(x_1, x_2\right) = \frac{2M_Z^4\left(\cos^2\alpha, \sin^2\alpha\right)}{\pi v^2 s\left(1-x_1-x_2-m_{h,H}^2/s+M_Z^2/s\right)^2} \times \left[\frac{m_{h,H}^2}{s} + \left(1-x_1\right)\left(1-x_2\right) - 2\left(1-x_1-x_2\right) + \frac{4m_t^2}{s}\right], \tag{B.18}$$

$$\begin{aligned} I_5\left(x_1, x_2\right) = {} & \frac{2M_Z m_t\left(\cos^2\alpha, \sin^2\alpha\right)}{\pi v^2}\frac{\left(2-x_1-x_2\right)}{\left(1-x_1\right)\left(1-x_2\right)\left(1-x_1-x_2-m_{h,H}^2/s+M_Z^2/s\right)} \\ & \times\left[\left(\left(1-x_1\right)\left(1-x_2\right) - \frac{m_{h,H}^2}{s}\right)\left(1-x_1-x_2-\frac{m_{h,H}^2}{s}\right) + \frac{m_t^2}{s}\left(\frac{12M_Z^2}{s} - \frac{4m_{h,H}^2}{s} + \left(2-x_1-x_2\right)^2\right)\right. \\ & \left. - \frac{3M_Z^2}{s}\left(\frac{m_{h,H}^2}{s} - \frac{2\left(1-x_1\right)\left(1-x_2\right)}{\left(2-x_1-x_2\right)}\right)\right], \end{aligned} \tag{B.19}$$

$$\begin{aligned} I_6\left(x_1, x_2\right) = {} & \frac{2M_Z^2 m_t^2\left(\cos^2\alpha, \sin^2\alpha\right)}{\pi v^2 s\left(1-x_1\right)\left(1-x_2\right)\left(1-x_1-x_2-m_{h,H}^2/s+M_Z^2/s\right)} \times\left[\left(2-x_1-x_2\right)\left(\frac{m_{h,H}^2}{s} - \frac{4m_t^2}{s} - 2\right)\right. \\ & \left. - 2\left(1-x_1\right)\left(1-x_2\right) + \left(2-x_1-x_2\right)^2\right], \end{aligned} \tag{B.20}$$

$$I_7(x_1,x_2) = \frac{\left[f\left(\theta',g_1'\right)\cos\alpha \mp g\left(\theta',g_1'\right)\sin\alpha\right]^2}{2\pi\left(1-x_1-x_2-m_{h,H}^2/s+M_{Z'}^2/s\right)^2}\left[\frac{m_t^2}{s}\left(\frac{4m_{h,H}^2}{s}-(2-x_1-x_2)^2-\frac{12M_{Z'}^2}{s}\right)\right.$$
$$\left.+\frac{m_t^2}{M_{Z'}^2}\left(\frac{4m_{h,H}^2}{s}-(2-x_1-x_2)^2\right)\left(1-x_1-x_2-\frac{m_{h,H}^2}{s}+\frac{M_{Z'}^2}{s}\right)\right], \tag{B.21}$$

$$I_8(x_1,x_2) = \frac{M_{Z'}^2\left[f\left(\theta',g_1'\right)\cos\alpha \mp g\left(\theta',g_1'\right)\sin\alpha\right]^2}{2\pi s\left(1-x_1-x_2-m_{h,H}^2/s+M_{Z'}^2/s\right)^2}\times\left[\frac{m_{h,H}^2}{s}+(1-x_1)(1-x_2)-2(1-x_1-x_2)+\frac{4m_t^2}{s}\right], \tag{B.22}$$

$$I_9(x_1,x_2) = \frac{M_Z m_t(\cos\alpha,\sin\alpha)\left[f\left(\theta',g_1'\right)\cos\alpha \mp g\left(\theta',g_1'\right)\sin\alpha\right]}{\pi v M_{Z'}}$$
$$\times\frac{(2-x_1-x_2)}{(1-x_1)(1-x_2)\left(1-x_1-x_2-m_{h,H}^2/s+M_{Z'}^2/s\right)}\times\left[\left((1-x_1)(1-x_2)-\frac{m_{h,H}^2}{s}\right)\left(1-x_1-x_2-\frac{m_{h,H}^2}{s}\right)\right. \tag{B.23}$$
$$\left.+\frac{m_t^2}{s}\left(\frac{12M_{Z'}^2}{s}-\frac{4m_{h,H}^2}{s}+(2-x_1-x_2)^2\right)-\frac{3M_{Z'}^2}{s}\left(\frac{m_{h,H}^2}{s}-\frac{2(1-x_1)(1-x_2)}{(2-x_1-x_2)}\right)\right],$$

$$I_{10}(x_1,x_2) = \frac{M_Z M_{Z'} m_t(\cos\alpha,\sin\alpha)\left[f\left(\theta',g_1'\right)\cos\alpha \mp g\left(\theta',g_1'\right)\sin\alpha\right]}{\pi v s(1-x_1)(1-x_2)\left(1-x_1-x_2-m_{h,H}^2/s+M_{Z'}^2/s\right)}\times\left[(2-x_1-x_2)\left(\frac{m_{h,H}^2}{s}-\frac{4m_t^2}{s}-2\right)\right.$$
$$\left.-2(1-x_1)(1-x_2)+(2-x_1-x_2)^2\right]. \tag{B.24}$$

Conflicts of Interest

The authors declare that there are no conflicts of interest regarding the publication of this paper.

Acknowledgments

The authors acknowledge support from SNI and PROFOCIE (Mexico). Alejandro González-Sánchez acknowledges the Research Department of UPAEP, where most of this work was carried on, for the hospitality and the access to all its resources.

References

[1] E. Accomando, A. Aranda, E. Ateser et al., "Physics at the CLIC Multi-TeV Linear Collider," *High Energy Physics - Phenomenology*, 2004.

[2] D. Dannheim, P. Lebrun, L. Linssen et al., "CLIC e+e- linear collider studies," *Physics*, 2012.

[3] H. Abramowicz, "Higgs physics at the CLIC electron-positron linear collider," *European Physical Journal*, vol. 77, no. 475, 2017.

[4] P. Higgs, "Broken symmetries, massless particles and gauge fields," *Physics Letters*, vol. 12, no. 2, pp. 132-133, 1964.

[5] P. W. Higgs, "Broken symmetries and the masses of gauge bosons," *Physical Review Letters*, vol. 13, pp. 508-509, 1964.

[6] F. Englert and R. Brout, "Broken symmetry and the mass of gauge vector mesons," *Physical Review Letters*, vol. 13, no. 9, article 321, 1964.

[7] G. S. Guralnik, "Naturally occurring zero-mass particles and broken symmetries," *Physical Review Letters*, vol. 13, pp. 295–298, 1964.

[8] T. W. B. Kibble, "Symmetry breaking in n-Abelian gauge theories," *Physical Review A: Atomic, Molecular and Optical Physics*, vol. 155, no. 5, pp. 1554–1561, 1967.

[9] S. Khalil, "Low-scale B##hssm###x2013;L extension of the standard model," *Journal of Physics G: Nuclear and Particle Physics*, vol. 35, no. 5, Article ID 055001, 2008.

[10] E. Osalusi, "Effects of thermal radiation on MHD and slip flow over a porous rotating disk with variable properties," *Romanian Journal of Physics*, vol. 52, no. 3-4, pp. 217–229, 2007.

[11] L. Basso, A. Belyaev, S. Moretti, and C. H. Shepherd-Themistocleous, "Phenomenology of the minimal *B–L* extension of the standard model: *Z* and neutrinos," *Physical Review D: Particles, Fields, Gravitation and Cosmology*, vol. 80, no. 5, Article ID 055030, 14 pages, 2009.

[12] L. Basso, A. Belyaev, S. Moretti et al., "Probing the Z*ı* sector of the minimal B-L model at future Linear Colliders in the e+e− ⟶ *μ*+*μ*− process," *Journal of High Energy Physics*, 2009.

[13] F. Ramírez-Sánchez, A. Gutiérrez-Rodríguez, and M. A. Hernández-Ruíz, "Higgs bosons production and decay at future e + e − linear colliders as a probe of the B–L model," *Journal of Physics G: Nuclear and Particle Physics*, vol. 43, no. 9, 2016.

[14] M. A. Hernández-Ruíz and A. Gutiérrez-Rodríguez, "Z' Resonance and Associated Zh Production at Future Higgs Boson Factory: ILC and CLIC," *Advances in High Energy Physics*, vol. 2015, Article ID 593898, 9 pages, 2015.

[15] L. Basso, A. Belyaev, S. Moretti et al., “Probing the Z’ sector of the minimal B−L model at future Linear Colliders in the e+e− ⟶ $\mu+\mu-$ process,” *Journal of High Energy Physics*, vol. 2009, 2009.

[16] J. Han et al., “Higgs boson production in the U(1)B−L model at the ILC,” *International Journal of Modern Physics A*, vol. 31, no. 17, Article ID 1650099, 2016.

[17] R. N. Mohapatra and G. Senjanovic, “Neutrino mass and spontaneous parity nonconservation,” *Physical Review Letters*, vol. 44, p. 912, 1980.

[18] R. N. Mohapatra and R. E. Marshak, “ Local ,” *Physical Review Letters*, vol. 44, no. 24, pp. 1644-1644, 1980.

[19] M. Jamil, D. Momeni, and M. A. Rashid, “Notes on dark energy interacting with dark matter and unparticle in loop quantum cosmology,” *The European Physical Journal C*, vol. 71, p. 1711, 2011.

[20] L. Basso, S. Moretti, and G. M. Pruna, “Constraining the g'_1 coupling in the minimal *B-L* model,” *Journal of Physics G: Nuclear and Particle Physics*, vol. 39, no. 2, Article ID 025004, 2012.

[21] L. Basso, S. Moretti, and G. M. Pruna, “Renormalization group equation study of the scalar sector of the minimal B-L extension of the standard model,” *Physical Review D: Particles, Fields, Gravitation and Cosmology*, vol. D82, 2010.

[22] L. Basso, *Phenomenology of the minimal B-L extension of the Standard Model at the LHC [Ph.D. Thesis]*, 2011, https://arxiv.org/abs/1106.4462.

[23] S. Iso, N. Okada, and Y. Orikasa, “Minimal *B−L* model naturally realized at the TeV scale,” *Physical Review D: Particles, Fields, Gravitation and Cosmology*, vol. 80, no. 11, Article ID 115007, 12 pages, 2009.

[24] A. Ferroglia, A. Lorca, and J. J. van der Bij, “The Z’ reconsidered,” *Annals of Physics*, vol. 16, no. 7-8, pp. 563–578, 2007.

[25] T. G. Rizzo, “Z’ Phenomenology and the LHC,” 2006, https://arxiv.org/abs/hep-ph/0610104.

[26] G. Aad, “ Erratum: Measurements of ,” *Physical Review D: Particles, Fields, Gravitation and Cosmology*, vol. 91, no. 11, 2015.

[27] S. Chatrchyan, V. Khachatryan, and A. M. Sirunyan, “Observation of a new boson at a mass of 125 GeV with the CMS experiment at the LHC,” *Physics Letters B*, vol. 76, no. 1, pp. 30–61, 2013.

[28] P. Bandyopadhyay, E. J. Chun, H. Okada, and J. C. Park, “Implications of right-handed neutrinos in B − Lextended standard model with scalar dark matter,” *Journal of High Energy Physics*, 2013.

[29] L. Basso, “A renormalization group analysis of the Hill model and its HEIDI extension,” *Physics Letters B*, vol. 730, no. 7, pp. 326–331, 2013.

[30] A. Gutiérrez-Rodríguez, in *Proceedings of the 20th International Conference on Particles and Nuclei (PANIC 14)*, A. Schmid and C. Sander, Eds., Hamburg, Germany, 2014.

[31] S. Y. Zhao, C. X. Yue, and Y. Yu, “The *HZZ*’ coupling and the Higgs-strahlung production $pp \longrightarrow ZH$ at the LHC,” *International Journal of Theoretical Physics*, vol. 55, no. 2, pp. 648–657, 2016.

[32] S. Schael, “Precision electroweak measurements on the Z resonance,” *Physics Reports*, vol. 427, no. 5-6, pp. 257–454, 2006.

[33] G. Cacciapaglia, C. Csáki, G. Marandella, and A. Strumia, “The minimal set of electroweak precision parameters,” *Physical Review D: Particles, Fields, Gravitation and Cosmology*, vol. 74, no. 3, Article ID 033011, 2006.

[34] E. Salvioni, G. Villadoro, and F. Zwirner, “Minimal *Z*’ models: present bounds and early LHC reach,” *Journal of High Energy Physics*, vol. 2009, no. 11, 68 pages, 2009.

[35] C. Patrignani, “Review of particle physics,” *Chinese Physics C*, vol. 40, no. 10, 2016.

[36] G. Aad, “Search for high-mass dilepton resonances in pp collisions at $\sqrt{s}$ = 8 TeV with the ATLAS detector,” *Physical Review D: Particles, Fields, Gravitation and Cosmology*, vol. 90, Article ID 052005, 2014.

[37] V. Khachatryan, A. M. Sirunyan, and A. Tumasyan, “Search for physics beyond the standard model in dilepton mass spectra in proton-proton collisions at $\sqrt{s}$=8 TeV,” *Journal of High Energy Physics*, vol. 1504, no. 25, 2015.

[38] V. Khachatryan, “Erratum: Search for single production of scalar leptoquarks in proton-proton collisions at $\sqrt{s}$ =8 TeV,” *Physical Review D: Particles, Fields, Gravitation and Cosmology*, vol. 91, no. 3, Article ID 052009, 2015.

[39] S. Banerjee, M. Mitra, and M. Spannowsky, “Searching for a heavy Higgs boson in a Higgs-portal *B-L* model,” *Physical Review D: Particles, Fields, Gravitation and Cosmology*, vol. 92, Article ID 055013, 2015.

[40] E. Accomando, C. Corianò, L. D. Rose, J. Fiaschi, C. Marzo, and S. Moretti, “$Z\prime$, Higgses and heavy neutrinos in U(1)$\prime$ models: from the LHC to the GUT scale,” *Journal of High Energy Physics*, vol. 2016, no. 7, 86 pages, 2016.

[41] A. Djouadi, J. Kalinowski, P. M. Zerwas, and Z. Phys, “Higgs radiation off top quarks in high-energy e+e− colliders,” *Zeitschrift für Physik C Particles and Fields*, vol. 54, no. 2, pp. 255–262, 1992.

[42] A. Djouadi, “The anatomy of electroweak symmetry breaking: tome I: the Higgs boson in the Standard Model,” *Physics Reports*, vol. 457, no. 1-4, pp. 1–216, 2008.

[43] S. Dawson and L. Reina, “QCD corrections to associated Higgs boson production,” *Physical Review D: Particles, Fields, Gravitation and Cosmology*, vol. 57, no. 9, pp. 5851–5859, 1998.

[44] B. Abelev, A. Abrahantes Quintana, and D. Adamová, “Strange particle production in proton–proton collisions at $\sqrt{s} = 0.9$ TeV with ALICE at the LHC,” *The European Physical Journal C*, vol. 71, p. 1594, 2011.

[45] P. S. Bhupal Dev, A. Djouadi, R. M. Godbole, M. M. Mühlleitner, and S. D. Rindani, “Determining the CP Properties of the Higgs Boson,” *Physical Review Letters*, vol. 100, no. 5, 2008.

[46] J. Heeck, “Unbroken B−L symmetry,” *Physics Letters B*, vol. 739, no. 12, pp. 256–262, 2014.

[47] M. Carena, A. Daleo, B. A. Dobrescu, and T. M. Tait, “Z’ gauge bosons at the Fermilab Tevatron,” *Physical Review D: Particles, Fields, Gravitation and Cosmology*, vol. 70, no. 9, 2004.

[48] M. Köksal, A. A. Billur, and A. Gutiérrez-Rodríguez, “Bounds on the Electromagnetic Dipole Moments through the Single Top Production at the CLIC,” *Advances in High Energy Physics*, vol. 2017, Article ID 6738409, 14 pages, 2017.

[49] Y. Özgüven, S. C. Inan, A. A. Billur et al., “Search for the anomalous electromagnetic moments of tau lepton through electron–photon scattering at CLIC,” *Nuclear Physics B*, vol. 923, pp. 475–490, 2017.

[50] M. Köksal, S. C. Inan, A. A. Billur et al., “Analysis of the anomalous electromagnetic moments of the tau lepton in γp collisions at the LHC,” *High Energy Physics - Phenomenology*, 2017, https://arxiv.org/abs/1711.02405.

[51] M. Köksal, A. A. Billur, A. Gutiérrez-Rodríguez et al., “Model-independent bounds probing on the electromagnetic dipole

moments of the τ-lepton at the CLIC," *High Energy Physics - Phenomenology*, pp. 1–38, 2018, https://arxiv.org/abs/1804.02373.

[52] A. Gutiérrez-Rodríguez, M. Köksal, A. A. Billur et al., "Studies on the anomalous magnetic and electric dipole moments of the tau-neutrino in pp collisions at the LHC," *High Energy Physics - Phenomenology*, pp. 1–20, 2017, https://arxiv.org/abs/1712.02439.

[53] A. A. Billur and M. Köksal, "Probe of the electromagnetic moments of the tau lepton in γ-γ collisions at the CLIC," *Physical Review D: Particles, Fields, Gravitation and Cosmology*, vol. 89, no. 3, Article ID 037301, 2014.

[54] I. Sahin and M. Koksal, "Search for electromagnetic properties of the neutrinos at the LHC," *Journal of High Energy Physics*, vol. 100, no. 3, pp. 1–11, 2011, https://arxiv.org/abs/1010.3434.

[55] J. A. Aguilar-Saavedra, R. D. Heuer, D. J. Miller et al., *Technical Design Report Part III: Physics at an e+e- Linear Collider*, TESLA, 2001.

[56] G. Petrucciani, "for the ATLAS and CMS Collaborations," *CMS CR-2017/144*, 2017.

[57] F. Bezrukov and M. Shaposhnikov, "Why should we care about the top quark Yukawa coupling?" *Journal of Experimental and Theoretical Physics*, vol. 120, no. 3, pp. 335–343, 2015.

[58] G. 't Hooft, "Naturalness, Chiral Symmetry, and Spontaneous Chiral Symmetry Breaking," *Recent Developments in Gauge Theories*, vol. 59, pp. 135–157, 1980.

[59] M. Sher, "Electroweak Higgs potential and vacuum stability," *Physics Reports*, vol. 179, no. 5-6, pp. 273–418, 1989.

[60] G. Degrassi, S. Di Vita, J. Elias-Miró et al., "Higgs mass and vacuum stability in the Standard Model at NNLO," *Journal of High Energy Physics*, vol. 1208, no. 98, 2012.

[61] F. Ramírez-Sánchez, A. Gutiérrez-Rodríguez, A. González-Sánchez, and M. A. Hernández-Ruíz, "CP violation Higgs-top coupling in the context of the B-L model at future *e+e−* colliders," In press.